Published in Journal of Applied Physics 73, issue 4, 1826-1831, 1993
which should be used for any reference to this work

Annealing kinetics of *a*-Si:H deposited by concentric-electrode rf glow discharge at room temperature

J. P. Conde,[a] K. K. Chan, J. M. Blum, and M. Arienzo
I.B.M. Research Division, T. J. Watson Research Center, P.O. Box 218, Yorktown Heights, New York 10598

P. A. Monteiro and J. A. Ferreira
Department of Physics, Instituto Superior Técnico, Av. Rovisco Pais 1, 1096 Lisboa Codex, Portugal

V. Chu[b]
Laboratoire de Physique des Interfaces et des Couches Minces, UPR A 0258-CNRS, Ecole Polytechnique-91128 Palaiseau-Cedex, France

N. Wyrsh[c]
Department of Electrical Engineering, Princeton University, Princeton, New Jersey 08544

The irreversible isothermal annealing of the as-deposited defects of hydrogenated amorphous silicon, *a*-Si:H, deposited at room temperature by concentric-electrode radio-frequency glow discharge is studied using dark and photoconductivity, space-charge limited current, and time-of-flight. The photoconductivity increases as a power law of the annealing time with exponent 0.8. The density of states at the Fermi level, measured by space-charge limited current, is inversely proportional to the annealing time. These results are compatible with bimolecular annealing kinetics. The dark conductivity obeys a Meyer–Nelder rule during the isothermal anneal.

I. INTRODUCTION

Studies of annealing kinetics have increasingly been recognized as valuable tools for understanding the physics of metastability and equilibrium processes in *a*-Si:H. The first report of the Staebler–Wronski effect[1] already suggested that light-induced degradation was reversible by annealing the light-soaked sample at 150 °C. Early studies of the hydrogen evolution and defect density in *a*-Si:H as a function of temperature[2] also showed that defects annealed out below 250 °C and were created above that temperature.

Ast and Drodski observed[3] an increase in the dark conductivity, σ_d, at 300 K of samples that were fast-quenched from 473 K. The isothermal annealing of this excess σ_d followed bimolecular kinetics with an activation energy $E_a \sim 0.9$ eV. More recently, Lee *et al.* reported[4] a kinetical study of the decay of the increase in the electron spin resonance (ESR) signal caused by light soaking. This decay obeyed second-order kinetics for the density of unpaired spins, N_s:

$$\frac{dN_s}{dt_a} = -\nu N_s^2, \tag{1}$$

$$\frac{1}{N_s(t_a)} - \frac{1}{N_s(0)} = \nu t_a , \tag{2}$$

where t_a is the annealing time. The bimolecular rate ν was found to be thermally activated $[\nu = \nu_0 \exp(-E_a/kT)]$ with activation energy $E_a = 1.1$ eV. The interpretation of these results was based on the prediction of charge transfer between pre-existing charged dangling bond defects,[4–6] which must be in the order of 10^{17} cm^{-3}. In this model, defect annealing corresponds to the thermal excitation of a charge from the neutral dangling bond followed by a lattice relaxation to form charged defects (during light soaking, charged defects trap electrons and holes during illumination, followed by a lattice relaxation to stabilize the resulting neutral dangling bond). The distribution of environments for these charged defects, such as variations in the nearest neighbor distance or in the bond angles, was thought to produce a distribution of barrier heights.[6–9] Power-law kinetics were again reported for the recovery of the photoconductivity, σ_{ph}, after light soaking by Eser,[10] who found that the recovery of σ_{ph} was a fifth-order reaction, with $\sigma_{ph} \propto t_a^{0.26}$ and $E_a = 1.35$ eV, by Qiu *et al.* who obtained[11] a power-law behavior for the mobility-lifetime product $\mu\tau \propto t_a^{0.11}$, and by Tzeng *et al.*[12]

Monomolecular kinetics for the annealing of light-induced defects, as described by the equations

$$\frac{dN_s}{dt_a} = -\nu N_s , \tag{3}$$

$$N_s(t_a) = N_s(0)\exp(-\nu t_a), \tag{4}$$

was proposed by Stutzmann, Jackson, and Tsai[13,14] who, in order to fit the experimental results, had to include in the model a distribution of activation energies $f(E)$ (with a spread $\sigma_E = 0.07$ eV around $E_{a0} = 1.1$ eV). This distribution of activation energies was again ascribed to the different structural environments of a given dangling bond. This mechanism involved the breaking of chemical bonds associated with atomic hydrogen diffusion. During defect an-

[a]Present address: Department of Physics, Instituto Superior Técnico, Av. Rovisco Pais 1, 1096 Lisboa Codex, Portugal.
[b]Present address: Instituto de Engenharia de Sistemas e Computadores, Rua Alves Redol, 1000 Lisboa, Portugal.
[c]Present address: Institute of Microtechnology, University of Neuchâtel, A. L. Bréguet 2, CH-2000 Neuchâtel, Switzerland.

nealing hydrogen moves away, allowing the two dangling bonds to recombine (during light soaking, the first step is weak-bond breaking followed by the stabilization of the dangling bonds via H migration). More recently, Matsuura found[15] that simple monomolecular kinetics [Eqs. (3) and (4)] sufficed to fit his isothermal annealing data.

Kakalios *et al.*[16-18] suggested that the annealing of both light- and thermally induced defects followed a stretched exponential curve. The stretch exponential relation is

$$\Delta N_s(t_a)=\Delta N_s(0)\exp[-(t_a/\tau)^{\beta}], \tag{5}$$

where $\Delta N_s(t_a)=N_s(t_a)-N_0$ and $\Delta N_s(0)=N_{eq}-N_0$, with N_0 being the initial as-deposited deep state density (at $t_a=0$) and N_{eq} the fully annealed deep state density (when $t\rightarrow\infty$). τ was found to be thermally activated,

$$\tau=\tau_0\exp(E_a/kT), \tag{6}$$

with $E_a\sim 0.9$–1.0 eV and the dispersion parameter β linearly dependent on the temperature ($\beta=T/T_0$, with $T_0\sim 600$ K). These authors suggested that this dispersive behavior resulted from a distribution of bond energies for the breaking of the silicon-hydrogen bond with E_a closely related to the activation energy for the diffusion of hydrogen, which is[19] ~ 1.5 eV. These same authors also mention that monomolecular kinetics with a distribution of activation energies could explain equally well[16] their experimental results.

Recently, Parsons *et al.* published[20] a study on the post-deposition relaxation of electronic defects in *a*-Si:H. They deposited *a*-Si:H at $T_s=40$ °C by reactive magnetron sputtering and performed isothermal annealing on the films. They observed "small but systematic" deviations from the stretched exponential behavior for σ_d both at short and long annealing times. They also measured the activation energy of the relaxation time of the annealing of σ_d, $E_a\sim 1.6$, 1.7 eV. These authors suggested that higher energies are necessary to anneal-out defects that change the Fermi-level position (thus influencing σ_d) than those that are measured via ESR. They also found that the annealing of as-deposited defects showed smaller activation energy and longer time constants than that of light-induced defects and attributed this difference to possible variations in the local microstructure in the neighborhood of the defects.

This article is a study of the irreversible isothermal annealing of the as-deposited defects in *a*-Si:H films deposited at room temperature by concentric-electrode plasma-enhanced chemical vapor deposition. First, it is shown that σ_d obeys a Meyer–Neldel rule, and second, that the annealing of as-deposited defects follows second order kinetics. Finally, a discussion of alternative mechanisms and of the possible microscopic mechanisms of the annealing of these defects in these films is presented.

II. EXPERIMENTAL PROCEDURES

A concentric-electrode plasma-enhanced chemical vapor deposition (CE-PECVD) reactor was used[21] to deposit the *a*-Si:H thin films. The reactor consists of a quartz tube, lined inside by a grounded, cylindrical electrode (anode), which functions as a counter electrode to a 13.56 MHz, radio-frequency (rf)-powered, paddle-shaped electrode placed near the center of the reactor (cathode). The substrate is placed on the cathode electrode. The cylindrical symmetry of the CE-PECVD reactor creates a plasma with a high degree of dissociation and very symmetric potential distribution. The combined effects of electron confinement and moderate ion bombardment result[21-23] in high-growth rate, high-density, and low-hydrogen content *a*-Si:H films.

TABLE I. Deposition conditions and physical properties of *a*-Si:H sample RT-2.

Flow rate (silane)	15 sccm
Total pressure	0.030 Torr
rf power[a]	80 W
Substrate temperature[b]	25 °C
Film thickness	0.70 μm
Film growth rate	5.8 Å/s
Optical band gap[c]	1.63 eV
Hydrogen content[d]	14%
SiH/SiH_2[e]	7
Refractive index[f]	3.4

[a]rf power corresponds to power densities of ~ 0.003 W cm^{-3} (with respect to the volume of the reactor) or of ~ 0.06 W cm^{-2} (with respect to the area of the powered electrode).
[b]Nominal temperature, real substrate temperature ~ 40 °C.
[c]Tauc's E_{opt}.
[d]Estimated form the integrated intensity of the stretching bands in the 2000–2100 cm^{-1} region.
[e]Corresponds to the ratio of α at 2000 and 2090 cm^{-1}.
[f]Extracted from the interference fringe spacing in the low absorption region below E_{opt}.

The *a*-Si:H sample used in this study was deposited at room temperature from silane. The deposition conditions and some physical properties of the as-deposited sample, prior to annealing, are indicated in Table I. These deposition conditions result in low hydrogen concentration and a dominant monohydride silicon-hydrogen bonding configuration. Quartz substrates were used for the optical transmission and conductivity measurements, while double-side-polished wafers were used for the infrared absorption measurements.

Cr electrodes were evaporated in a coplanar gap structure (0.2 cm wide, 1.0 cm long) for conductivity measurements parallel to the film surface. These contacts were found to be ohmic for the voltages applied (~ 100 V). σ_{ph} was measured using bandpass filtered illumination from a tungsten-halogen lamp adjusted to yield an approximately uniform volume carrier generation rate, G, of 10^{21} cm^{-3} s^{-1}. The photoconductivity γ factor was measured from the intensity dependence of σ_{ph} ($\sigma_{ph}\propto G^{\gamma}$) using calibrated neutral density filters, such that G varied from 10^{17} to 10^{21} cm^{-3} s^{-1}. The activation energies $E_{a,d}$ and $E_{a,ph}$, of σ_d and σ_{ph}, respectively, were extracted from the temperature dependence of σ_d and σ_{ph} in the temperature range between 300 and 400 K, using $\sigma_d=\sigma_{0,d}\exp(-E_{a,d}/kT)$ and $\sigma_{ph}=\sigma_{0,ph}\exp(-E_{a,ph}/kT)$, respectively, where $\sigma_{0,d}$ and $\sigma_{0,ph}$ are the pre-exponential factors of σ_d and σ_{ph}, respectively. The isothermal anneal was performed in a furnace under nitrogen flow. The samples were quenched

to room temperature for measurement after a given annealing time.

The determination of the density of states at the Fermi level, $g(E_F)$, was made using the space-charge-limited-current technique[24] (SCLC). The measurement took place with the sample in the sandwich configuration with the bulk film between n-type crystalline Si on one side and Cr contacts on the other. Using the analytical approach of Solomon *et al.*, i.e., by fitting,[25] the theoretical SCLC dimensionless current-voltage (I-V) curves to the experimental data, one is able to extract the parameters V_c (the transition voltage at which the current goes from the ohmic to the space-charge-limited regime) and l ($l=T_g/T$, where T_g characterizes the electron trap distribution in $g(E)=N_g \exp[-(E_c-E)/kT_g]$, and E_c is the energy of the conduction-band edge). Using these two parameters, $g(E_F)$ can be calculated using $V_c=eg(E_F)kTld^2$ (where e is the electronic charge, and d is the thickness of the sample).

The drift mobility, $\mu_{d,h}$, and the drift mobility-deep trapping lifetime product, $(\mu_d\tau_d)_h$ for holes were determined by the time-of-flight technique[26,27] on Schottky barriers formed with 10-nm-thick semitransparent Pd dots. The breakpoint of the log-log plot of the photocurrent versus time is the transit time, t_T, from which the drift mobility can be calculated ($\mu_h=d^2/Vt_T$, where V is the externally applied voltage). The total collected charge Q (the integrated photocurrent) can be plotted versus V and fitted to the Hecht expression[28] to extract $(\mu_d\tau_d)_h$.

III. RESULTS

Isothermal annealing was performed on the as-deposited sample at three temperatures, T_a, respectively, 107, 160, and 200 °C. The kinetics of the isothermal annealing were followed using several optoelectronic characterization techniques, namely σ_d, σ_{ph} [measured as a function of the temperature (σ_d and σ_{ph}) and carrier generation rate (σ_{ph})], SCLC, and time-of-flight.

A. Dark conductivity

Figure 1 shows σ_d as a function of t_a for the three annealing temperatures. σ_d remains approximately constant at $\sigma_d \sim 10^{-10}\ \Omega^{-1}\ \mathrm{cm}^{-1}$ for $T_a=107$ and 160 °C. For $T_a=200$ °C, σ_d drops slightly from $\sim 6\times10^{-11}$ to $\sim 3\times10^{-11}\ \Omega^{-1}\ \mathrm{cm}^{-1}$ as $t_a \to 10^5$ s. Figure 2 shows the variation of $E_{a,d}$ with t_a. For all annealing temperatures, an approximately linear increase of $E_{a,d}$ with $\ln t_a$ is observed, $E_{a,d}$ increasing ~ 0.08 eV from the initial, nonannealed, state as $t_a \to 10^5$ s.

Figure 3 is a plot of $E_{a,d}$ as a function of the logarithm of $\sigma_{0,d}$. The experimental points for the three T_a fall on the same straight line, thus obeying a Meyer–Neldel rule (MNR).[29] To our knowledge, this is the first observation of a MNR behavior in which the variation of $E_{a,d}$ has been experimentally followed, in a single sample, by annealing of the as-deposited defects. The fit to the MNR rule, $\sigma_d=\sigma_{00}\exp(BE_{a,d})\exp(-E_{a,d}/kT)$, indicated in Fig. 3 yields $B=38.5\ \mathrm{eV}^{-1}$ and $\ln\sigma_{00}=-23$. Note that the Meyer–Neldel slope,[30,31] $B=1/kT_0$ is approximately equal

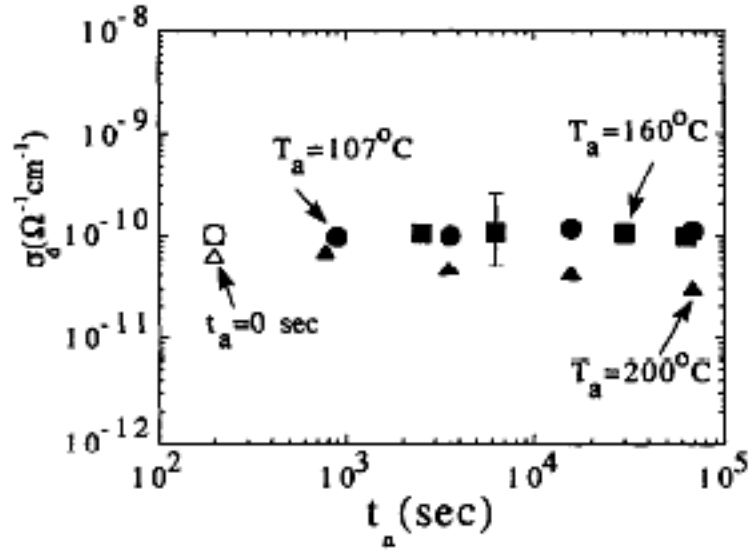

FIG. 1. Dark conductivity, σ_d, measured at room temperature (300 K) plotted as a function of the annealing time, t_a. The annealing temperatures, T_a were 107 (●), 160 (■), and 200 °C (▲). The open symbols correspond to the initial, nonannealed values for σ_d measured at $t_a=0$ s. σ_d stays approximately constant with t_a.

to the value of $1/kT$ at room temperature. When this happens, $\sigma_d \sim \sigma_{00}$ is approximately constant and independent of the particular value of $E_{a,d}$, as is the case in Fig. 1. σ_{00} is directly related to the intrinsic extended state mobility μ_0, which should remain approximately constant during annealing, and the product $\exp(BE_{a,d})\exp(-E_{a,d}/kT)$ is proportional to $\exp[-(E_C-E_F)]$ thus indicating that E_F remains approximately constant during isothermal annealing of the as-deposited defects. This conclusion is in good agreement with the observation of a nearly constant σ_d during annealing (Fig. 1), which would yield a constant E_C-E_F if one considered a constant pre-exponential factor.

The current models for the MNR[30–32] rely on the statistical shift of the Fermi energy with temperature in a region with a steep slope of the density of states (DOS). Although the Meyer–Nelder behavior is not sensitive to the details of the DOS, physically unrealistic values of high

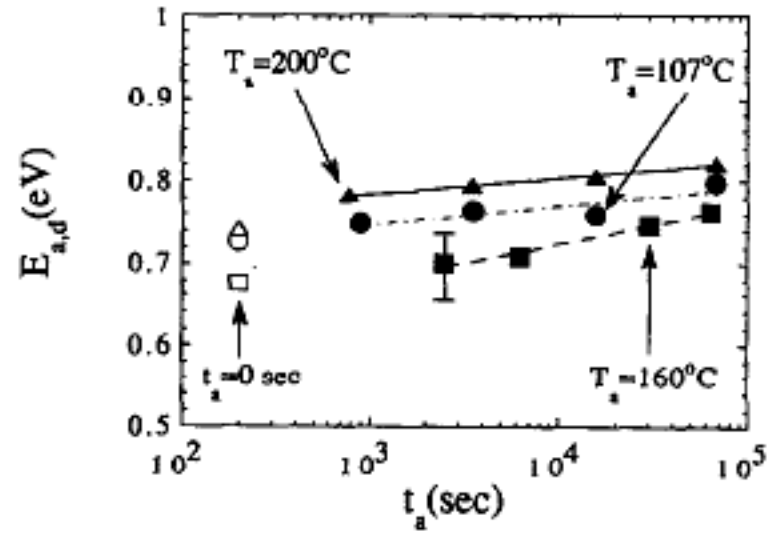

FIG. 2. Activation energy, $E_{a,d}$, from $\sigma_d=\sigma_0\exp(-E_{a,d}/kT)$ plotted as a function of the annealing time, t_a. The measurement temperature range was between 20 and 60 °C. The straight lines are least square fits to the data (for $t_a>0$).

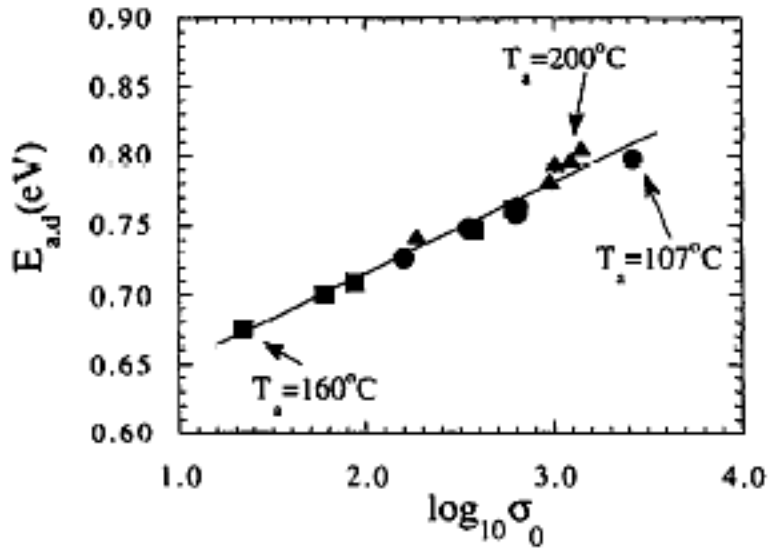

FIG. 3. Plot of $E_{a,d}$ as a function of the pre-exponential factor, σ_0, of σ_d [$\sigma_d=\sigma_0\exp(-E_{a,d}/kT)$], showing a proportionality between the $\log_{10}\sigma_0$ and $E_{a,d}$ (i.e., σ_d obeys a Meyer-Neldel rule).

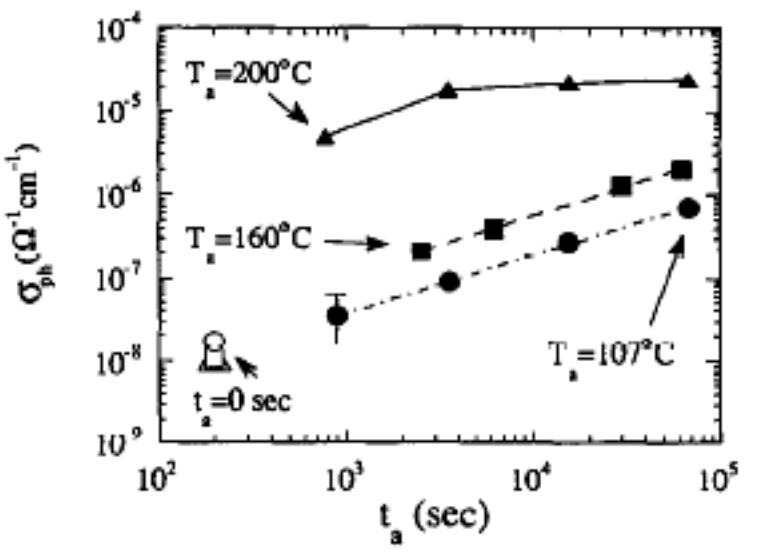

FIG. 4. Photoconductivity, σ_{ph}, measured at room temperature and under a generation rate $G\sim10^{21}$ cm^{-3} s^{-1} using approximately uniformly absorbed light plotted as a function of the annealing time, t_a. Notice the power-law relationship $\sigma_{ph}\propto t_a^{\delta}$ for $T_a=107$ and 160 °C ($\delta\simeq0.8$) and the saturation behavior observed for $T_a=200$ °C. The full line (for $T_a=200$ °C, $t_a>0$) joins the experimental points.

σ_{00} and low B are expected if the density of gap states changes substantially during the experiment.[33] In this work, the value of the MNR slope, B, translates[33] into a slope of an exponential tail state distribution of $G\sim B/0.6=64$ eV^{-1}, which is high compared with typically observed values of 25–40 eV^{-1} and σ_{00} is correspondingly lower. This behavior suggests that in the annealing of the as-deposited states in CE-PECVD a-Si:H a large decrease of the density of gap states may occur.

In early papers by Spear[33,34] it was shown that for films deposited by rf glow discharge at substrate temperatures below 350 K, the transport is dominated by holes hopping in localized states near the valence-band edge, while for higher deposition temperatures the transport mechanism involves electrons in extended states above the conduction-band edge. At the transition temperature between these two regimes, these authors observed an increase of $E_{a,d}$, a minimum of σ_d and an increase in the pre-exponential factor σ_0 similar to what is observed in Figs. 1 and 2. Measurements of $(\mu_d\tau_d)_h$ during isothermal annealing at $T_a=135$–140 °C show a reduction of $(\mu_d\tau_d)_h$ from $\sim3\times10^{-8}$ cm^2 V^{-1} for $t_a=2.6\times10^3$ s to $\sim4\times10^{-9}$ cm^2 V^{-1} for $t_a=9\times10^4$ s. This reduction of $(\mu_d\tau_d)_h$ is in agreement with the hypothesis of a changeover in the majority carrier.

B. Photoconductivity

Figure 4 shows a strong variation of σ_{ph} with t_a. After $t_a\sim10^5$ s, σ_{ph} showed an increase of approximately three orders of magnitude for $T_a=200$ °C and of two orders of magnitude for $T_a=107$ °C. For $T_a=107$ and 160 °C, σ_{ph} clearly obeys a power-law dependence on t_a, $\sigma_{ph}\propto t_a^{\delta}$, while for $T_a=200$ °C, a saturation of σ_{ph} is already reached at $t_a>3\times10^3$ s. A least-square fit of $\sigma_{ph}(t_a)-\sigma_{ph}(0)$ results in a slope of $\delta=0.73$ for $T_s=160$ °C and $\delta=0.84$ for $T_s=107$ °C. Figure 5 shows a plot of $E_{a,ph}$ as a function of $\ln t_a$. An approximately linear decrease in $E_{a,ph}$ for $T_a=107$ and 160 °C is observed, while for the sample annealed at 200 °C, saturation behavior is observed for $t_a>10^3$ s in agreement with the results of Fig. 4. Figure 6 shows that γ drops abruptly ($\Delta\gamma\sim0.1$) after an initial annealing period ($t_a\sim10^3$ s) and then levels off at ~0.8, remaining approximately independent of t_a for $t_a>10^3$ s.

According to the model of Rose,[35] when $\gamma\sim0.5$, one is in the presence of recombination through shallow traps, whereas when $\gamma\sim1.0$, region recombination proceeds through the deep states. In general, an intermediate situation is found in a-Si:H, with $0.5<\gamma<1.0$. According to the model proposed by Rose, γ is related to the slope of the density of states, kT_c (at the energy range over which the electron quasi-Fermi level, E_{Fn}, is swept by varying the generation rate G or the temperature), by the relation $\gamma=kT_c/(kT+kT_c)$. The sharp drop in γ observed in Fig. 6 suggests that, before annealing, E_{Fn} moves in a region of approximately constant density of states ($kT_c>kT$) and, by the time the first experimental point after the beginning

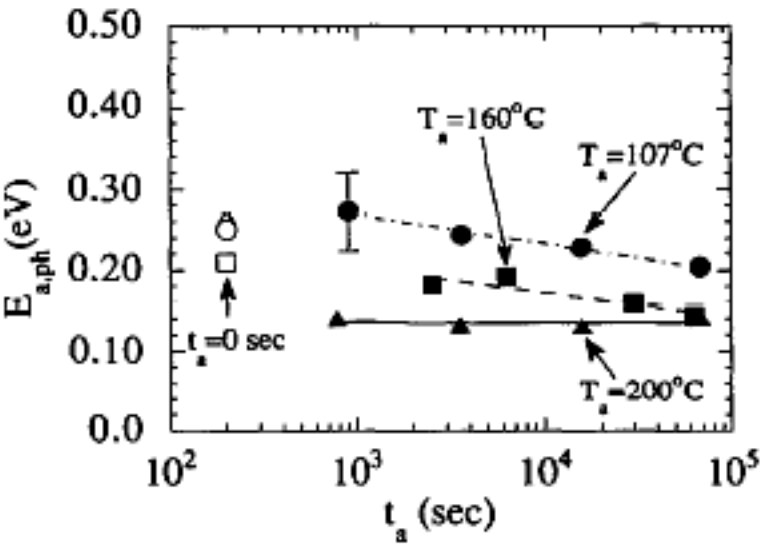

FIG. 5. Activation energy, $E_{a,ph}$, of σ_{ph} plotted as a function of the annealing time, t_a [$\sigma_{ph}\propto\exp(-E_{a,ph}/kT)$]. Measurements of σ_{ph} were performed between 20 and 60 °C at a generation rate $G\sim10^{21}$ cm^{-3} s^{-1}. $E_{a,ph}$ decreases as the annealing proceeds. The straight lines are least-square fits of the experimental data (for $t_a>0$).

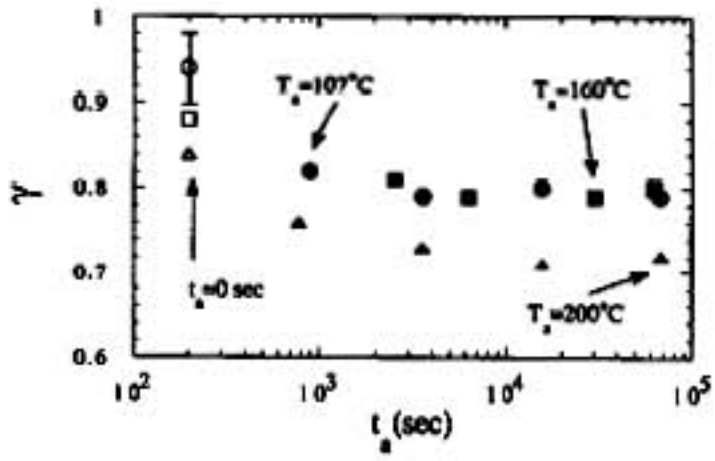

FIG. 6. Photoconductivity γ factor ($\sigma_{ph} \propto G^{\gamma}$, where G is the carrier generation rate) plotted as a function of the annealing time, t_a. γ was measured at room temperature while G was varied between 10^{17} and 10^{21} $cm^{-3}s^{-1}$. A sharp drop of γ is observed with annealing, followed by saturation at $\gamma \sim 0.8$.

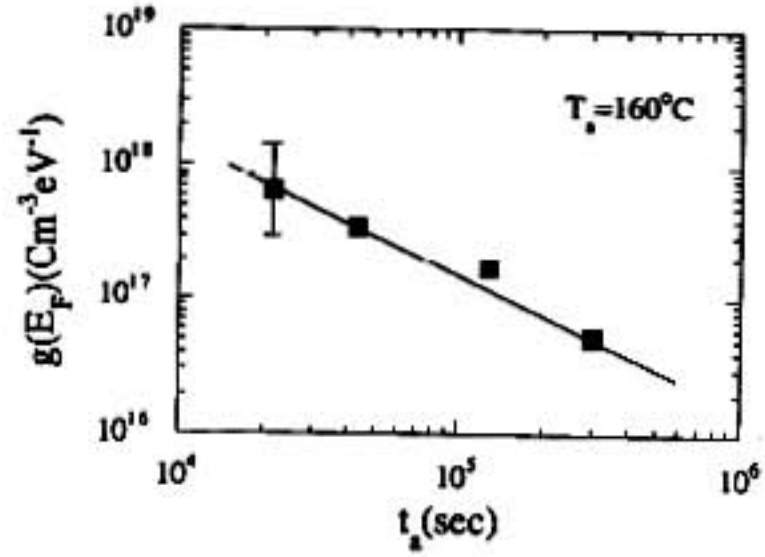

FIG. 7. Density of states at the Fermi level, $g(E_F)$, for a sample annealed at 160 °C measured by the SCLC technique. The straight line shown has a slope of -1 (showing that the experimental results follow $1/g(E_F) \propto t_a$).

of the isothermal annealing was taken, at $t_a \sim 10^3$ s, E_{Fn} was already scanning the midgap side of the $D^{0/-}$ peak[37] ($kT_c \sim 0.1$ eV). This behavior suggests either a sharp drop in the midgap density of states or a Fermi level shift, or both. $E_{a,ph}$, γ, and $E_C - E_{F,n}$ are, in a first order approximation[36] to the Rose model of σ_{ph}, related by $E_{a,ph} = (E_C - E_{F,n})(1-\gamma)$. For $t_a > 0$, γ remains approximately constant, so the small decrease in $E_{a,ph}$ must be attributed to an increase in the Fermi level splitting during illumination ($E_F - E_{Fn}$), which is in turn compatible with a reduction in the defect density in the energy range scanned by E_{Fn} during annealing.

A theoretical method based on the Rose photoconductivity model shows[37] that the photosensitivity σ_{ph}/σ_d is a power law of the deep defect density N_s with exponent $-\gamma$

$$\frac{\sigma_{ph}}{\sigma_d} \propto N_s^{-\gamma}. \tag{7}$$

Since σ_d remains constant throughout the isothermal annealing and $\sigma_{ph}(t_a>0) \gg \sigma_{ph}(t_a=0)$, one can replace Eq. (7) into Eq. (2), and obtain $\sigma_{ph} \propto t_a^{\gamma}$, in good agreement with the results in Fig. 4, in which σ_{ph} showed a power-law dependence on t_a with $\delta \sim \gamma \sim 0.8$. Note that this result does not strictly require a constant σ_d. Indeed, the same result would have been obtained if σ_{ph} had been replaced by the photosensitivity σ_{ph}/σ_d, as long as $[\sigma_{ph}/\sigma_d](t_a>0) \gg [\sigma_{ph}/\sigma_d](t_a=0)$.

C. SCLC

A plot of $g(E_F)$ resulting from the analysis of I-V characteristics showing space-charge-limited current as a function of annealing times is given in Fig. 7. Also shown in this figure is a straight line with slope of -1. The experimental results are clearly compatible within the experimental error to $1/g(E_F) \propto t_a$. If the total deep defect density N_s is proportional to the density of states at the Fermi level $g(E_F)$, this behavior confirms the bimolecular model presented before in which $1/N_s \propto t_a$ [Eqs. (1) and (2)] [if $N_s(t_a>0) \ll N_s(t_a=0)$]. The proportionality between N_s and $g(E_F)$ will also occur if the density of states retains the same overall shape during annealing, in which case a MNR is expected. The simple picture[13,37] that σ_{ph} proportional to $1/N_s$ or to $1/N_s^2$ has been challenged.[38] Although the variations in the photoconductivity may reflect changes in the recombination rate constant rather than changes in the defect density, the self-consistency revealed by the SCLC and the σ_{ph} measurements is a confirmation of the applicability of the models used above[37] relating N_s and σ_{ph} to this particular situation.

IV. DISCUSSION

The microscopic mechanism resulting in bimolecular kinetics for annealing consists of the simultaneous removal of a pair of dangling bonds with local formation of a weak bond. A monomolecular process is to be expected in the context of the bond-breaking model for the Staebler–Wronski effect.[13] In this case, although two dangling bonds are needed for bond formation, monomolecular kinetics are still followed if the two dangling bonds involved are statistically correlated.[39,40] In order for bimolecular kinetics to be observed, any statistical correlation between this pair of dangling bonds must be eliminated. This can happen if the pair is free to migrate throughout the amorphous network.[39] In light of these arguments, it is likely that the as-deposited condition ensures that the dangling bonds involved in the annealing process are not statistically correlated. A bimolecular mechanism for the irreversible isothermal annealing of the as-deposited defects will occur in these films if one assumes random locations for the as-deposited defects.[4]

From a fitting of the data in Fig. 4 using bimolecular kinetics, we obtain values for the activation energy of ν of $E_a = 1.15 \pm 0.1$ eV in reasonable agreement with previous studies[4,9,10,41] of annealing of light-induced defects. A fit of the data in Figs. 4 and 7 using monomolecular kinetics [Eqs. (3) and (4)] was also attempted, but the experimental results could not be fitted. A bimolecular model with a distribution of annealing energies was also tried, but the

quality of the fit did not improve significantly with respect to that using a bimolecular model with a single activation energy.

An attempt to fit the results presented in Figs. 4 and 7 using a stretched exponential (or, equivalently, using monomolecular kinetics with a distribution of annealing energies) was also performed. No good fitting could be achieved, but the limited set of experimental data available does not allow a definitive conclusion based solely on these results. The best adjusted curves result in a β that is approximately independent of temperature and $\sim 0.18 \pm 0.2$. The activation energy for τ was approximately 1.1 ± 0.2 eV. K decreased from 2.4 for $T_a = 200$ °C to 0.68 for $T_a = 107$ °C ($K = \tau^{-\beta}$). Note the small relaxation time, $\tau_0 \sim 10^{-14}$ s, when compared to the values in the literature, which are typically[41] between 10^{-12} and 10^{-10} s. On the other hand, Xu *et al.* point out[42] that when they alloy with carbon or nitrogen, the relaxation time increases. They suggest that the longer relaxation time results because a larger defect density in the alloys should be associated with a broader distribution of hydrogen bonding energies, which is responsible for the dispersive behavior. Early papers on dispersive transport suggested that a temperature-independent β could be the result of tunneling or hopping carrier transport to the defect site.[43,44] More recently, a nearly temperature-independent value of β was measured for *a*-Si:H samples deposited using dc sputtering and a decrease in the apparent activation energy of τ with respect to a glow discharge sample (1.8 eV) was attributed[45,46] to a phonon-assisted hydrogen tunneling process. The source of the observed dispersive behavior was attributed to fluctuations in the wave-function overlap integral between the states involved in the hopping process. The low value of β, which appears to be independent of temperature, would indicate[45,47] that the annealing process is due to a tunneling transport mechanism in this temperature range and not multiple trapping. This observation is compatible with the high N_s present in the initial state of films deposited at room temperature.

V. CONCLUSIONS

The irreversible annealing of the as-deposited defects of CE-PECVD *a*-Si:H samples deposited at room temperature was found to follow second-order kinetics. Although one should be careful not to mistake the molecularity for the order of the reaction,[10] these results suggest an annealing process in which a pair of statistically uncorrelated dangling bonds (present in the film as as-deposited defects at random locations in the film) is simultaneously removed with formation of a Si–Si chemical bond. No need was found to invoke dispersive behavior in this particular annealing situation.

ACKNOWLEDGMENTS

The authors gratefully acknowledge Professor Sigurd Wagner of Princeton University and Dr. Bernard Equer of the LPICM of Ecole Polytechnique for the use of their respective laboratories.

[1] D. L. Staebler and C. R. Wronski, Appl. Phys. Lett. **31**, 292 (1977).
[2] D. K. Biegelsen, R. A. Street, C. C. Tsai, and J. C. Knights, Phys. Rev. B **20**, 4839 (1979).
[3] D. G. Ast and M. H. Brodsky, Proceedings of the 14th International Conference on the Physics of Semiconductors, Edinburgh, 1978, edited by B. C. H. Wilson, p. 1159.
[4] C. L. Lee, W. D. Ohlsen, P. C. Taylor, H. S. Ullal, and G. P. Ceasar, Phys. Rev. B **31**, 100 (1985).
[5] D. L. Staebler and C. R. Wronski, J. Appl. Phys. **51**, 3262 (1980).
[6] R. S. Crandall, Phys. Rev. B **43**, 4057 (1991).
[7] M. Campos and J. A. Giacometti, Appl. Phys. Lett. **34**, 226 (1979).
[8] Y. Bar-Yam, D. Adler, and J. D. Joannopolus, Phys. Rev. Lett. **57**, 467 (1988).
[9] R. S. Crandall, Phys. Rev. B **36**, 2645 (1987).
[10] E. Eser, J. Appl. Phys. **59**, 3508 (1986).
[11] C. Qiu, W. Li, and D. Han, J. Appl. Phys. **64**, 713 (1988).
[12] W. J. Tzeng, H. K. Tsai, and S. C. Lee, J. Appl. Phys. **62**, 1856 (1987).
[13] M. Stutzmann, W. B. Jackson, and C. C. Tsai, Phys. Rev. B **32**, 23 (1985).
[14] M. Stutzmann, W. B. Jackson, and C. C. Tsai, Phys. Rev. B **34**, 63 (1986).
[15] H. Matsuura, Appl. Phys. Lett. **54**, 344 (1989).
[16] J. Kakalios, R. A. Street, and W. B. Jackson, Phys. Rev. Lett. **59**, 1037 (1987).
[17] W. B. Jackson and J. Kakalios, Phys. Rev. B **37**, 1020 (1988).
[18] W. B. Jackson, J. M. Marshall, and M. D. Moyer, Phys. Rev. B **39**, 1164 (1989).
[19] D. E. Carlson and C. W. Magee, Appl. Phys. Lett. **33**, 81 (1978).
[20] G. N. Parsons, C. Wang, M. J. Williams, and G. Lucovsky, Appl. Phys. Lett. **56**, 1895 (1990).
[21] J. P. Conde, K. K. Chan, J. M. Blum, M. Arienzo, and J. J. Cuomo, J. Appl. Phys. **71**, 3981 (1992).
[22] T. Hamasaki, M. Ueda, A. Chayahara, M. Hirose, and Y. Osaka, Appl. Phys. Lett. **44**, 600 (1984).
[23] J. Perrin, Pure Appl. Chem. **62**, 1681 (1990).
[24] W. den Boer, J. Phys. (Paris) Colloq. **42**, C4-451 (1981).
[25] I. Solomon, R. Benferhat, and H. Tran-Quoc, Phys. Rev. B **30**, 3422 (1984).
[26] R. A. Street, Phys. Rev. B **27**, 4924 (1983).
[27] T. Tiedje, in *Hydrogenated Amorphous Silicon Device Applications*, Vol. 21, Part C, *Semiconductors and Semimetals*, edited by J. I. Pankove (Academic, New York, 1984), p. 207.
[28] K. H. Hecht, Z. Phys. **77**, 235 (1932).
[29] W. Meyer and H. Neldel, Z. Tech. Phys. **18**, 588 (1937).
[30] H. Overhof and W. Beyer, Philos. Mag. **47**, 377 (1983).
[31] G. Oversluizen, R. P. van Kessel, K. J. Nieuwesteeg, and J. Boogaard, J. Appl. Phys. **69**, 3082 (1991), and references therein.
[32] F. Djamdji and P. G. LeComber, Philos. Mag B **56**, 31 (1987).
[33] W. E. Spear, Adv. Phys. **23**, 523 (1974)
[34] W. E. Spear, *Proceedings of the 5th International Conference on Amorphous and Liquid Semiconductors*, edited by J. Stuke and W. Brenig (Taylor and Francis, London, 1974), p. 1.
[35] A. Rose, *Concepts in Photoconductivity and Allied Problems* (Interscience, New York, 1963).
[36] J. Z. Liu and S. Wagner, Phys. Rev. B **39**, 11156 (1989).
[37] S. Aljishi, Z E. Smith, and S. Wagner, *Amorphous Silicon and Related Materials*, edited by H. Fritzsche (World Scientific, Singapore, 1988), p. 887.
[38] E. Bhattacharya, A. H. Mahan, R. S. Crandall, and J. I. Pankove, Appl. Phys. Lett. **54**, 1247 (1989).
[39] W. B. Jackson and M. Stutzmann, Appl. Phys. Lett. **49**, 957 (1986).
[40] E. Z. Liu and W. E. Spear, Adv. Phys. **23**, 523 (1974)
[41] R. A. Street and K. Winer, Phys. Rev. B **40**, 6236 (1989).
[42] X. Xu, H. Sasaki, A. Morimoto, M. Kumeda, and T. Shimizu, Phys. Rev. B **41**, 10049 (1990).
[43] H. Scher and E. W. Montroll, Phys. Rev. B **12**, 2455 (1975).
[44] G. Pfister and H. Scher, Phys. Rev. B **15**, 2062 (1977).
[45] R. Meaudre, P. Jensen, and M. Meaudre, Phys. Rev. B **38**, 12449 (1988).
[46] M. Meaudre, P. Jensen, and R. Meaudre, Philos. Mag. B **63**, 815 (1991).
[47] E. D. Tober, J. Kanicki, and M. S. Crowder, Appl. Phys. Lett. **59**, 1723 (1991).